Baghdad Science Journal

Volume 23 | Issue 2 Article 23

2-23-2026

Green Synthesis and Characterization of Prepared Copper Iodide (CuI) Nanoparticles Using Red Cabbage Extract

A. S. Abd-Alsada
Department of Physics, College of Science for Women, University of Baghdad, Iraq,
amanysameer530@gmail.com

Zainab J. Shanan
Department of Physics, College of Science for Women, University of Baghdad, Iraq,
zainabjs_phys@csw.uobaghdad.edu.iq

Aqel Mashot Jafar
Renewable Energy Directorate, Solar Energy Center, Ministry of Higher Education and Scientific Research/ Science and Technology, Baghdad, Iraq, aqel.mashot@gmail.com

How to Cite this Article

Abd-Alsada, A. S.; Shanan, Zainab J.; and Jafar, Aqel Mashot (2026) "Green Synthesis and Characterization of Prepared Copper Iodide (CuI) Nanoparticles Using Red Cabbage Extract," *Baghdad Science Journal*: Vol. 23: Iss. 2, Article 23.
DOI: https://doi.org/10.21123/2411-7986.5215

BAGHDAD SCIENCE JOURNAL 2026;23(2):678–687

RESEARCH ARTICLE

Green Synthesis and Characterization of Prepared Copper Iodide (CuI) Nanoparticles Using Red Cabbage Extract

A. S. Abd-Alsada [1], Zainab J. Shanan [1], Aqel Mashot Jafar [2,*]

[1] Department of Physics, College of Science for Women, University of Baghdad, Iraq
[2] Renewable Energy Directorate, Solar Energy Center, Ministry of Higher Education and Scientific Research/Science and Technology, Baghdad, Iraq

ABSTRACT

Copper iodide nanoparticles, CuI NPs, are one of the promising materials for use in many electronic applications. In this work, transparent CuI nanoparticles were prepared by the green force synthesis, which was done by red cabbage extract used not only as a reduction but also as a capping agent to reduce the toxicity in the preparation of CuI nanostructures. The structural properties were investigated by the X-ray diffraction analysis technique, XRD. The X-ray analysis shows the structure has a polycrystalline nature with a cubic phase and appears to have a preferential orientation direction along the (111) plane. Atomic force microscopy surface morphology, AFM, of CuI thin film was used to examine and measure the morphology, average diameter and roughness. The optical measurements were confirmed by UV-Visible, which showed the CuI nanoparticles have a directly allowed energy gap and a change in absorbance to a shorter wavelength (to Ultraviolet wavelength shifted region). The Fourier Transform infrared spectroscopy, FT-IR, verified the presence of C=O, N-O and C-H bonds, this study confirms the high reducing and capping capacity of CuI NPs via biomolecules found in the plant extract. Field emission scanning electron microscopy, FE-SEM, analysis displayed the morphology of the CuI NPs, the results showed images of the produced copper iodide nanoparticles appear to be sheets of triangular flakes. The distribution pattern of CuI NPs particle size and stability was studied using a zeta potential analyzer. Zeta sizer analysis revealed -5.08 mV zeta potential demonstrating poor stability because of the accumulation of the material.

Keywords: Copper iodide, Green synthesis, Red cabbage extract, Morphological characteristics, Optical properties

Introduction

Recently, nanotechnology has been applied due to its properties based on structure and various phenomena. They display a specific surface area and size-dependent quantum confinement effects and appear in different shapes and sizes, leading to unique quantum properties. They possess distinctive electrical, optical, magnetic, catalytic, and thermal characteristics compared to macro-sized particles.[1] On this basis, copper-based nanoparticles have been widely studied due to their natural abundance and simple and low-cost manufacturing methods.[2,3] CuI NPs are metal semiconductors that occur naturally as a mineral called “marshite”. It may also be produced via redox interactions of copper and iodine.[4] It is a p-type semiconductor with remarkable optical features, and due to its remarkable qualities, it has been used in a wide variety of technical applications.[5] It is known as I-VII because Cu and I are numbered one and seven on the periodic Table, respectively. CuI NPs are one of the most exciting p-type material prospects because of their wide conductivity range, which allows them to be used in optoelectronic

Received 21 May 2024; revised 27 December 2024; accepted 29 December 2024.
Available online 24 February 2026

* Corresponding author.
E-mail addresses: amanysameer530@gmail.com (A. S. Abd-Alsada), Zainabjs_phys@csw.uobaghdad.edu.iq (Z. J. Shanan), aqel.mashot@gmail.com (A. M. Jafar).

https://doi.org/10.21123/2411-7986.5215

devices such as transparent electrodes and semiconducting layers in solar cells.[6] On the other hand, transparent copper halides, CuI, provide wide optical band gaps, Eg > 3.1 eV, and high hole mobility, up to 44 $cm^2 V^{-1}. s^{-1}$, with p-type Conductivity, reaches 280 $S.cm^{-1}$, thanks to its broad range of hole concentrations, 10^{16} to 10^{20} cm.[3,7,8] Several studies have investigated the application of CuI as a hole transport layer for perovskite solar cells. Khadka et al. established that the shape of the CuI film markedly affects the properties of the perovskite layer applied over it. CuI-based perovskite solar cells demonstrated superior stability to those utilizing PEDOT: PSS, with an efficiency of roughly 14.21%.[9] In a significant work, Sun et al. attained a remarkable power conversion efficiency (PCE) of 4.15% with copper iodide (CuI)-based polymer solar cells (PSCs), which exhibited enhanced air stability relative to PSCs utilizing PEDOT: PSS as a hole transport layer (HTL).[10] Moreover, researchers have concentrated on altering the HTL with CuI to improve perovskite solar cell efficacy. By interposing CuI between the perovskite layer and PTAA, they enhanced the crystallization of the perovskite film, yielding a remarkable efficiency of 20.34%, which significantly exceeds the 17.7% efficiency attained by devices utilizing PTAA exclusively.[11] The Green synthesis of nanoparticles is a bottom-up approach in which the nanoparticles are produced by the oxidation and reduction process, which provides several benefits over chemical and physical methods: non-toxic, pollution-free, ecologically friendly, and more sustainable.[12–15] Fernandez et al.[16] investigated the green synthesis of copper iodide nanoparticles utilizing anthocyanin-rich bean seed extract. They examined the characteristics of the produced copper iodide using powder X-ray diffraction and scanning electron microscopy. By powder X-ray diffraction and scanning electron microscopy, the size of CuI was determined to be in the nanoscale range. The produced copper iodide precipitated as Nanoflowers. The synthesized CuI had significant antibacterial action.[16] Prior research indicated that copper iodide nanoparticles (CuI NPs) synthesized by green methods have been investigated utilizing bean seed extract. Nonetheless, prior research has not examined the application of red cabbage extract, a rich source of anthocyanins, which are water-soluble pigments functioning as reducing, capping, and stabilizing agents in nanoparticle synthesis.[17,18] In the present article, the authors describe their work on preparing copper iodide nanoparticles (CuI NPs) synthesized by a green method utilizing red cabbage extract.

Furthermore, most prior research has focused on the green production of copper iodide nanoparticles (CuI NPs) for antimicrobial purposes. They have employed structural and antibacterial assays for many bacterial models. Previous research has not examined the manufacture of copper iodide nanoparticles for solar cell applications; therefore, this work presents a green synthesis approach for fabricating copper iodide nanoparticles intended for solar cell materials. Structural tests were conducted to verify the material's purity. Optical examinations were conducted to investigate the absorption, energy gap, and light interaction with the material. Zeta potential assessments were conducted to investigate the assembly mechanism of copper iodide nanoparticles (CuI NPs).

Experimental part

Green synthesis was used to prepare copper iodide nanoparticles in a practical part of the synthesis. Red cabbage extract was prepared by mixing, 20 gm, of red cabbage leaves with, 200 ml, of distilled water and placed under a magnetic stirrer for 30 minutes at room temperature. The resulting paste was filtered using medical gauze, and centrifugation was used to remove the largest amount of filtrate to obtain a pure extract of red cabbage to manufacture copper iodide nanoparticles. For prepared copper iodide nanoparticles, (30 ml) of red cabbage extract was added drop-wise to, 0.3 M, of Copper Sulfate solution. Then this mixture was stirred for 30 minutes at room temperature. After that, potassium iodide solution, 0.2 M, was added drop-wise to "the mixture of extract and $CuSO_4$" and stirred for 30 minutes at room temperature. The centrifuge was used to wash the resulting substance several times using 96% ethanol and distilled water. Finally, the resultant material was sifted through filter paper and dried in the air. The end product is a yellowish-white powder, as shown in Fig. 1.

Results and discussion

The XRD diffractometer pattern of CuI NPs products prepared by the green synthesis using red cabbage extract was reported to crystallize in a polycrystalline structure and cubic phases of Nano-crystalline cuprous iodide. The film was deposited for examination using a drop-casting method on the glass substrate, JCPDS card number, 82-2111. In Fig. 2, the peak position in the XRD pattern of the prepared film appeared at (111), (220), and (311) directions with high intensity, proving the high crystallinity of products synthesized by this method and without any impurity, at the orientation of 2θ degrees values: 24.9182°,41.7791°, and 49.5279° respectively. The

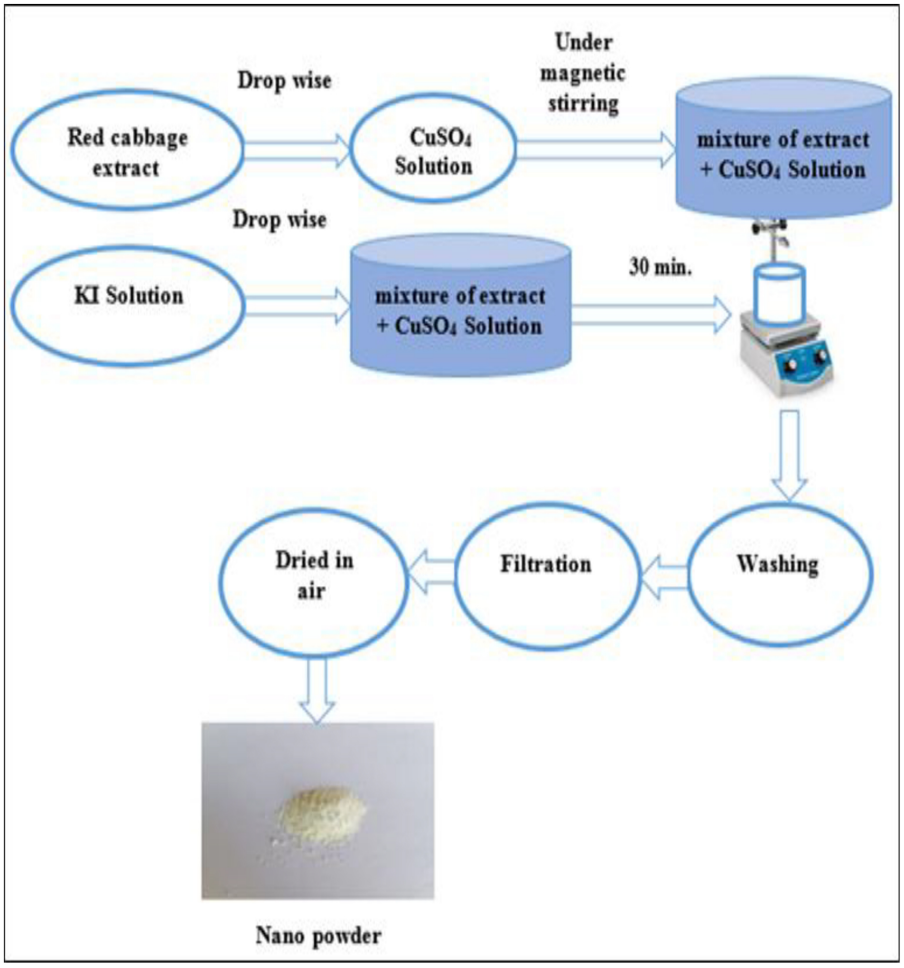

Fig. 1. Synthesis of copper iodide nanoparticles via the green method.

position of other reflection peaks were observed at (200), (400), (331), and (422) at (2θ) degrees values, which include 28.9432°, 61.3140°, 67.0202°, and 76.7947° respectively. The peaks of CuI NPs were observed to be broadened with low intensity at 51.9291° and 69.6780°, which include (222), and (420), respectively; this is consistent with research. [19,20] There is a difference between these degrees and those in the literature, which occurred because of different crystalline orientations formed due to various production methods. However, it is necessary to realize that the broadening of various peaks arises mainly due to instrumental effects, crystallite size, and lattice strain. The best sample crystallinity appeared for (111) and (220) orientations. The biggest crystal size of CuI NPs observed in the film formed is 35.88 nm, while the smallest was observed as 21.07 nm in the film.

The film's crystalline size, C. S., was determined using the Debye-Scherrer formula. The Scherrer equation estimates the, C.S., by measuring the full width of the diffraction peak at half maximum intensity, FWHM, [21]:

$$C.S = \frac{K.\lambda}{\beta\ coscos\ \theta} \quad (1)$$

Where $C.S$ = size of crystallite, nm,

- κ = The Scherrer constant dependent on crystallite shape = 0.94,
- λ = XRD wavelength, mostly λ for Cu-Kα =1.54056 A°,

β is the instrumental-corrected total width of the reflection, measured in radius. It indicates the increasing width or band of the hkl diffraction peak at half-height, measured in radians, θ, and hkl refer to the Bragg diffraction peak angle and Millar coefficients, respectively, as shown in Table 1. In general, crystallite size, C.S., measures the size coherence diffraction domain, which operates as a polycrystalline aggregate. The Crystallite size is not the same as particle size; often, it is smaller. Many methods are

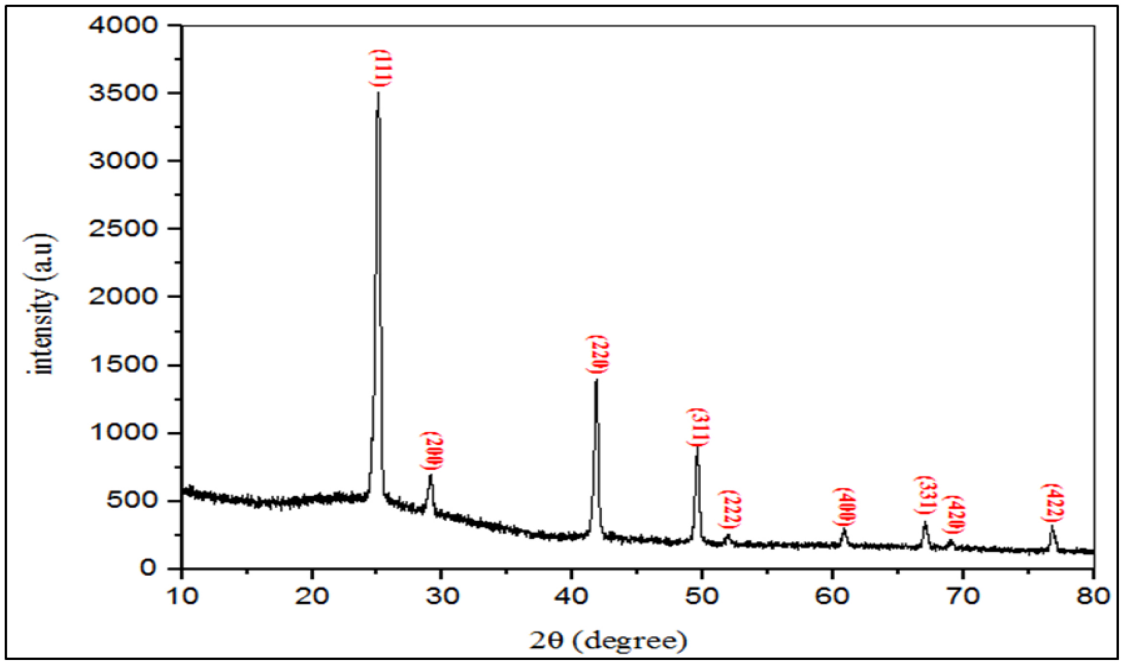

Fig. 2. The XRD pattern of CuI thin film.

available in the literature to calculate lattice strain; from those methods, "Williamson and Hall" are most commonly used.[22] We can symbolize the crystal size very simply as $B_{crystalline}$ So:[21]

$$B_{hkl} = B_{Crystallite} + B_{Strain} \quad (2)$$

The relationship can represent the broadening due to lattice strain in the material:[23]

$$B_{Strain} = 4\eta \, tantan \, \theta \quad (3)$$

Where, η, is the strain in the material. Hence, we can write that:[21]

$$B_{hkl} = \frac{k\lambda}{\beta coscos \, \theta} + 4\eta \, tantan \, \theta \quad (4)$$

Rearranging equation, 3, we get:[21]

$$B_{hkl} coscos \, \theta = \frac{k\lambda}{\beta} + 4\eta \, sinsin \, \theta \quad (5)$$

Eq. (5) is the Williamson and Hall relationship.[21] Table 1 indicates that the most excellent crystal size, determined using the Debye-Scherrer formula, is C. S. = 32 nm at the (331) plane and a position of 2θ = 67.0202°. The most excellent lattice strain occurs at the (400) crystal plane.

Fig. 3a illustrates atomic force microscope images, AFM, and their granularity accumulation distribution for CuI NPs thin film, which was prepared by the drop-casting method and deposited on glass substrates at 25 °C. The average diameter of the CuI grains was about 46.10 nm; Root Mean Square, RMS = 1.18 nm, and Roughness Average, RA = 0.865 nm. We note from Fig. 3a that the distribution of nanoparticles changes where the structure has become vertical. This result can be explained by the accumulation of CuI NPs, which leads to aggregation among them and the formation of large nanoparticles.

Fig. 3a. Illustrates atomic force microscope images, AFM, and their granularity accumulation distributions for CuI NPs thin films, which were prepared by the drop-casting method and deposited on glass substrates at 25 °C. The average diameter of the CuI grains was about 46.10 nm; Root Mean Square, RMS = 1.18 nm, and Roughness Average, RA = 0.865 nm. We note from the figure that the distribution of nanoparticles changes where the structure has become vertical. This result can be explained by the agglomeration of CuI NPs, which leads to aggregation among them and the formation of large nanoparticles. Therefore, the green method for synthesizing copper iodide nanoparticles is essential in creating thin films composed of Nano-CuI with nanoscale particle size dimensions suitable for applying thin films to prepare solar cells.

The optical properties of deposited CuI thin film have been determined by (UV-VIS-NIR) absorption spectroscopy in 100-1100 nm. Fig. 4. illustrates the absorption peak that appeared at around 230 nm, suggesting CuI NPs formation. In the spectra, the

Table 1. XRD parameters for CuI thin film analysis data.

2θ(degree)	FWHM 2θ, radius	d-spacing, Å	C.S., nm	(h,k,l)	Lattice strain
24.9182°	0.3155	3.57045	25.8524	(111)	1.01648
28.9432°	0.2574	3.54463	31.9537	(200)	0.50802
41.7791°	0.3546	2.16031	24.0336	(220)	0.39752
49.5279°	0.3275	1.83894	26.7690	(311)	0.30807
51.9291°	0.3500	1.75942	25.2966	(222)	0.31844
61.3140°	0.43904	1.5107	21.0704	(400)	1.71662
67.0202°	0.2933	1.39526	32.5337	(331)	0.26677
69.6780°	0.42150	1.35991	22.9953	(420)	0.0038
76.7947°	0.2828	1.24019	35.8814	(422)	0.15593

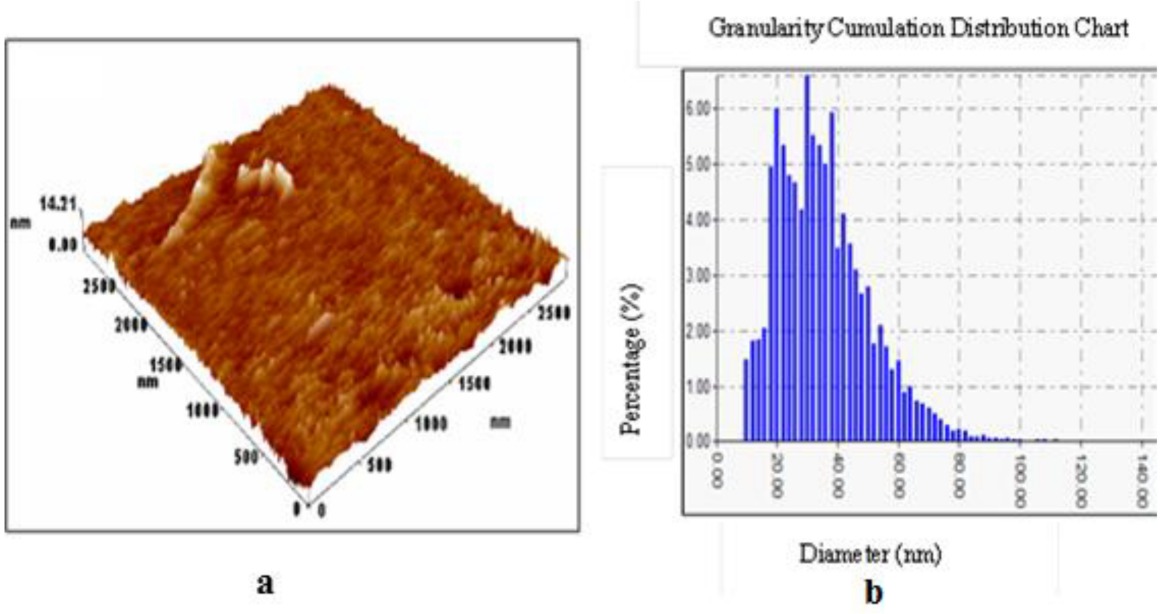

Fig. 3. a, AFM 3D-image for a thin film of CuI NPs. b, Shows a chart plot of grain size percentage for the Gaussian distribution of CuI NPs.

peak is attributed to the shift in surface plasmon resonance (SPR) resulting from the absorption of nanoparticles.[22] The particles' "SPR" peaks vary with the reaction media's size, shape, and dielectric constant.

The crystallite of the film structure may be responsible for the alterations in the absorption spectra to shorter wavelengths and higher energy states. It can also be attributed to a reduction in particle size, which increases the direct optical band gap due to the quantum confinement effect.[23] The film's optical energy gap (Eg = 3.1 eV), has been calculated based on the absorption coefficient data, as shown in Fig. 4b, which varies with photon energy, hυ in eV. Based on the (Planck relation) $E_{g=\frac{h\upsilon}{\lambda max}}$.

h represents Planck's constant, whereas the symbol υ represents the frequency.

Fig. 4 shows that the absorbance of Nano-CuI thin films is low in the visible light spectrum 400-800 nm, i.e., they are transparent and allow the passage of visible light, which makes them suitable for solar cell applications. The thin films have a high energy gap (Eg = 3.1 electron volts), which makes them act as a voltage barrier that increases the capacity of solar cells, so Nano-CuI films are suitable for solar cell applications.

The Fourier transform infrared (FTIR) spectroscopy is used to analyze band structure at a wavenumber range, 400 – 4000 $cm^{-1,}$ to identify structural changes that may occur in samples. Fig. 5. depicts FT-IR spectra of red cabbage extract and CuI NPs. The broad and intense band at 3414 cm^{-1} corresponds to O–H and N–H stretching vibrations due to absorbed water. This result means the alkyl group is present in the system, indicating phenols and proteins in the extract.[24] The presence of an intense band positioned between 428 and 609 cm^{-1} is related to the Cu–I vibrations, confirming the presence of CuI as a crystalline structure.[25] The peaks at 2922, 2852, 1348, and 1236 cm^{-1} represent alkanes' C–H stretch. The carbonyl stretching vibration band, C=O of saturated aliphatic ketones, emerges at 1645.28 cm-1, commonly

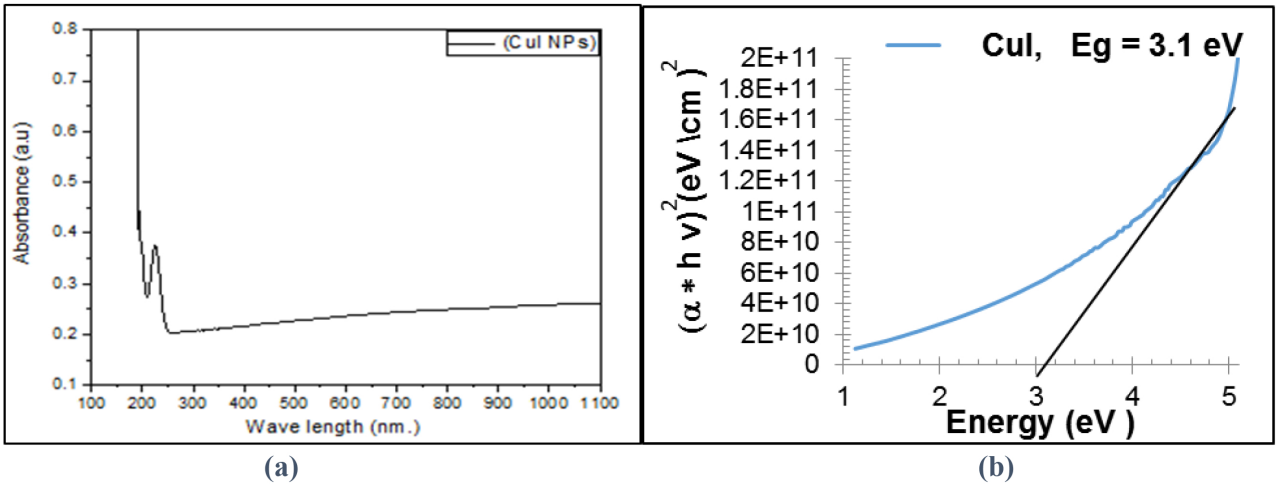

Fig. 4. (a). Absorbance Vs. Wavelength, (b) optical energy gap for CuI nanoparticles

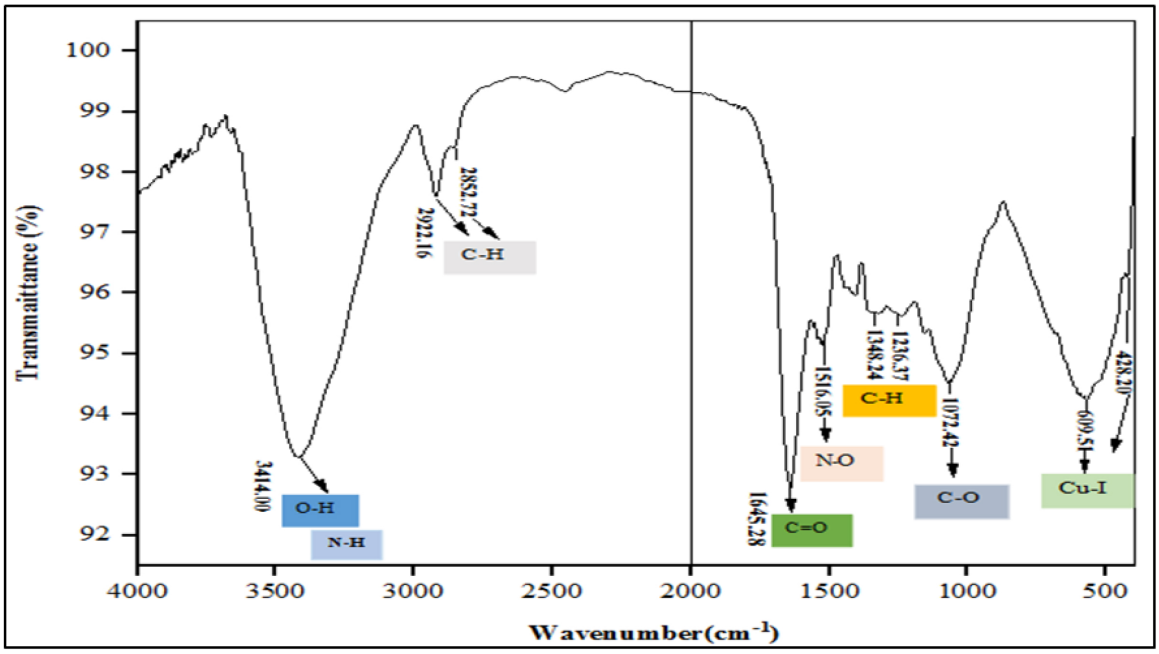

Fig. 5. FT-IR Spectrum of CuI NPs.

observed in protein. The C–H and C=O bonds present in plant extracts are responsible for reducing CuI precursors and capping CuI NPs.[26] The peak at 1516.05 cm^{-1} is assigned to N–O stretch vibration, which represents the nitroxide group,[27] and the bands at 1072.42 cm^{-1} were due to the stretching of the C–O bond,[28] which were absorbed at the surface of CuI, respectively.

Thus, this study confirms the strong reducing and capping ability of red cabbage extract of nanoparticles and the presence of certain functional groups, which was demonstrated by FTIR analysis of CuI NPs. Capping agents are critical in stabilizing nanoparticles and capped CuI NPs of phytochemicals present in the leaf extract. All the wavenumber of peaks and the band types are inserted in Table 2.

Fig. 6a. shows the morphology of the synthesized CuI particles studied using field emission scanning electron microscopy, FE-SEM, at 15.0 kV. FE-SEM was tested at scale-bar 1 μm and 200 nm magnification to observe the particle shape. The FE-SEM images indicate that the created CuI nanoparticles exhibit triangular flakes of CuI nanostructures that were practically produced. Fig. 6b. A particle size distribution histogram determined from the FE-SEM images showed a significant variation in the parti-

Table 2. Assignments of peak band in Fourier transform infrared (FT-IR) spectra of CuI NPs and red cabbage extract.

Type of band and assignment	Wavenumber (cm^{-1})	Reference
-OH stretch vibration of the phenolic	3414.00	20
C-H stretching vibration	2922, 2852.	22
C=O bending stretching vibration	1645	22
N-O stretching vibration	1516	23
C-H bending	1348, 1236	22
C-O stretching vibration	1072	24
Cu-I stretches	609, 428	21

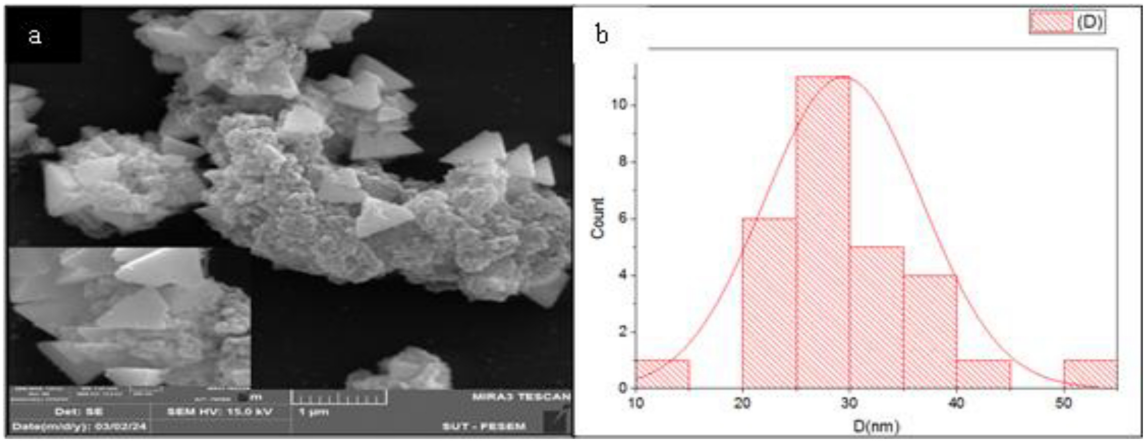

Fig. 6. (a) FE-SEM images of the nanostructures synthesized using the drop-casting method. (b) Practical size distribution histogram for the synthesis of CuI NPs.

cle size, where the average particle size was about 29 nm.

The stability, Conductivity, and dispersion of produced CuI NPs were examined using zeta potential tests. The zeta potential value of the CuI NPs is shown in Fig. 7. This result indicates that the synthesized green CuI NPs were relatively modest due to the material's accumulation as a result of the heat used in preparing the film and the medium-level electrostatic repulsion between the molecules. Because the particles have low values of zeta potential, they tend to flocculate or aggregate, which results in unstable

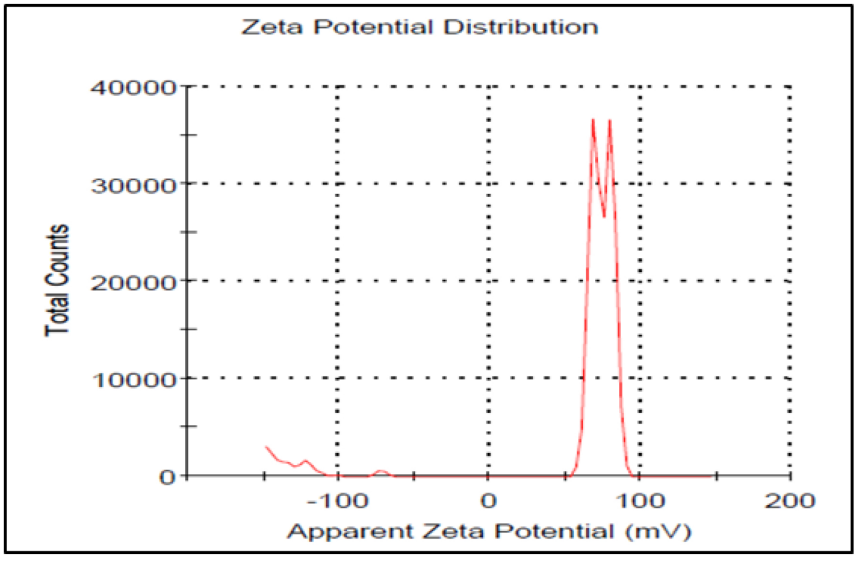

Fig. 7. Zeta potential of CuI NPs.

delivery systems. On the other hand, if the systems have a large positive or negative zeta potential, they will have a tendency to repel each other, indicating no affinity to flocculate or aggregate. For that reason, zeta potential is considered a crucial parameter for the delivery systems stability evaluation, being well accepted that its absolute value should be greater than 30 mV to ensure complete electrostatic stabilization.

Conclusion

In this study, CuI nanoparticles were produced using green synthesis utilizing red cabbage extract as the major reductant and capping agent. The XRD analysis reveals that the CuI structure is polycrystalline and exhibits a cubic formation. The optimal crystallinity of the sample was observed at the (111) orientation. The FE-SEM micrographs revealed a distinct and coarse microstructure characteristic of stacked triangles, with an average particle size of approximately 29 nm. Additionally, Atomic Force Microscopy data corroborated that the average diameter of CuI grains was around 46.10 nm. The investigation of optical properties reveals that the absorption coefficient of CuI thin films is low and semi-transparent, while the optical band gap of CuI thin films is a direct electronic transition, with an estimated value of Eg = 3.1 eV. FTIR study verifies the remarkable capacity of red cabbage for reduction and capping, evidenced by the presence of organic bonds indicative of plant organic components encasing the inorganic CuI particles. The organic bonds comprise C=O, C-O, C-H, N-O, O-H, N-H, C-H, and the inorganic bond CuI consists of Cu-I. The zeta potential of the synthesized CuI indicated a moderate value, resulting in the aggregation of the nanoparticles.

Acknowledgment

The cooperation of the Department of Physics, College of Science for Women, University of Baghdad -the authors appreciate Iraq.

Authors' declaration

- Conflicts of Interest: None.
- We hereby confirm that all the Figures and Tables in the manuscript are ours. Furthermore, any Figures and images, that are not ours, have been included with the necessary permission for republication, which is attached to the manuscript.
- No animal studies are present in the manuscript.
- No human studies are present in the manuscript.
- Ethical Clearance: The project was approved by the local ethical committee at the University of Baghdad.

Authors' contribution statement

A. S. A. A., and Z. J. Sh. contributed to the design and implementation of the research, the analysis of the results, and the writing of the manuscript, and A. M. J. contributed to the design and submission of the paper with input from all authors.

References

1. Khan I, Saeed K, Khan I. Nanoparticles: Properties, applications and toxicities. Arab J Chem. 2019;12(7):908–31. https://doi.org/10.1016/j.arabjc.2017.05.011.
2. Evano G, Blanchard N, Toumi M. Copper-mediated coupling reactions and their applications in natural products and designed biomolecules synthesis. Chem Rev. 2008;108(8):3054–131. https://doi.org/10.1021/cr8002505.
3. B R Baig N, S Varma R. Copper modified magnetic bimetallic nano-catalysts ligand regulated catalytic activity. Curr Org Chem. 2013;17(20):2227–37. https://doi.org/10.2174/13852728113179990045.
4. Zhao F, Zhang D, Xiaoe X, Mechanics F, Zhang L. Luminescence Properties and Mechanisms of CuI Thin Films Fabricated by Vapor Iodization of Copper Films. Materials. 2016;9(12). https://doi.org/10.3390/ma9120990.
5. Dhere SL, Latthe SS, Kappenstein C, Mukherjee SK, Rao AV. Comparative studies on p-type CuI grown on glass and copper substrate by SILAR method. Appl Surf Sci. 2010;256(12):3967–71. https://doi.org/10.1016/j.apsusc.2010.01.058.
6. Liu A, Zhu H, Kim M, Kim J, Noh Y. Engineering Copper Iodide (CuI) for Multifunctional p-Type Transparent Semiconductors and Conductors. Adv Sci. 2021;8(14):1–19. https://doi.org/10.1002/advs.202100546.
7. Yang C, Knei M, Lorenz M, Grundmann M. Room-temperature synthesized copper iodide thin film as degenerate p-type transparent conductor with a boosted figure of merit. Proc Natl Acad Sci U S A. 2016;113(46):12929–12933. https://doi.org/10.1073/pnas.1613643113.
8. Grundmann M, Schein F-L, Lorenz M, Böntgen T, Lenzner J, H v W. Cuprous iodide–ap-type transparent semiconductor. Hist Nov Appl. 2013;210(9):1671–703. https://doi.org/10.1002/pssa.201329349.
9. Abass NK, Alaubydi MA, Ulwali RA. Preparation, characterization of inorganic copper iodide nanoparticales using pomegranate juice extract and applications preparation, characterization of inorganic copper iodide nanoparticales using pomegranate juice extract, Plant Archives. 2020;20(1):2333–2340.
10. Olenic L, Chiorean I. Synthesis, characterization and application of nanomaterials based on noble metallic nanoparticles and anthocyanins. Mater Sci Chem. 2015;4(2):16–22.
11. Shanan ZJ, Hadi SM, Shanshool SK. Structural analysis of chemical and green synthesis of cuo nanoparticles and their effect on biofilm formation. Baghdad Sci J. 2018;15(2):211–216. https://doi.org/10.21123/bsj.2018.15.2.0211.

12. Shanan ZJ, and Shanshool SK. Nickel Oxide Nanoparticles: Synthesis and Evaluation for Antimicrobial Efficacy. Int. J. Nanosci. 2023;2350008. https://dx.doi.org/10.1142/S0219581X23500084.
13. Wessinger CA, Rausher MD, Bitonti MB. Lessons from flower colour evolution on changes targets of selection In Posidonia oceanica cadmium induces in DNA methylation and chromatin patterning. J Exp Bot. 2012;63(16):5741–9. https://doi.org/10.1093/jxb/err313.
14. Wessinger CA, Rausher MD, Bitonti MB. Lessons from flower colour evolution on changes targets of selection In Posidonia oceanica cadmium induces in DNA methylation and chromatin patterning. J Exp Bot. 2012;63(16):5741–9. https://doi.org/10.1093/jxb/err313.
15. Malekshahi M, Kharat A. Triangular-like cuprous iodide nanostructures: green and triangular-like cuprous iodide nanostructures: green and rapid synthesis using sugar beet juice. Rom J Biochem. 2014;51(2):101–107.
16. Fernandez AC, KM A, Rajagopal R. Green synthesis, characterization, catalytic and antibacterial studies of copper iodide nanoparticles synthesized using Brassica oleracea var. capitata f. rubra extract. Chem Data Collect. 2020;29:100538. Available from: https://doi.org/10.1016/j.cdc.2020.100538.
17. Cohen M. Elements of x- ray differaction, hand book, second eddition, 1978.
18. Access O. A comparative assessment of crystallite size and lattice strain in differently cast A356 aluminium alloy A comparative assessment of crystallite size and lattice strain in differently cast A356 aluminium alloy. IOP Conference Series: Materials Science and Engineering. 2015;75(1). https://doi.org/10.1088/1757-899X/75/1/012001.
19. Chowdhury PS, Sarkar A, Mukherjee P, Gayathri N, Bhattacharya M, Barat P. Studies of microstructural imperfections of powdered Zirconium-based alloys. Mater Charact. 2010;61(11):1061–5. Available from: http://dx.doi.org/10.1016/j.matchar.2010.06.019.
20. Cui J, Chen C, Han J, Cao K, Zhang W, Shen Y, *et al.* Surface plasmon resonance effect in inverted perovskite solar cells. Adv Sci. 2016;3(3):1–8. https://doi.org/10.1002/advs.201500312.
21. Borah P, Siboh D, Kalita P, Sarma J. Quantum Confinement Induced Shift in Energy Band Edges and Band Gap of Spherical Quantum Dot. Phys B: Condens Matter. 2017;530(1):208–214. https://doi.org/10.1016/j.physb.2017.11.046.
22. Ghanbari M, Bazarganipour M, Salavati-Niasari M. Photodegradation and removal of organic dyes using cui nanostructures, green synthesis and characterization. Sep Purif Technol. 2017;173:27–36. Available from: http://dx.doi.org/10.1016/j.seppur.2016.09.003.
23. Humud HR, Kadhem SJ, Khudhair DM. Structural and optical properties of copper iodide nanoparticles synthesized by electro-explosion of wire. J Chem Pharm Res. 2017;9(1):31–6.
24. Abdullah SH, Humud HR, Abood MA. Effect of current intensity on structural properties of cupper iodine nanoparticles produced by exploding Cu wire. Iraqi J Sci. 2019;17(41):1–6. https://doi.org/10.30723/ijp.v17i41.449.
25. Tavakoli F, Salavati-niasari M. A facile synthesis of CuI-graphene nanocomposite by glucose as a green capping agent and reductant. J Ind Eng Chem. 2013;(3):3170–3174. https://doi.org/10.1016/j.jiec.2013.11.061.
26. Humud HR, Kadhem SJ, Khudhair DM. Structural and optical properties of copper iodide nanoparticles synthesized by electro - explosion of wire. J Chem Pharm Res. 2017;9(1):31–6.
27. Yogalakshmi KMAD, Rajagopal R. Application of green synthesized nanocrystalline CuI in the removal of aqueous Mn (VII) and Cr (VI) ions. SN Appl Sci. 2019;1(6):1–14. https://doi.org/10.1007/s42452-019-0544-y.
28. Tsai L, Chen C, Lin C, Ho Y, Mi F. Development of mutlifunctional nanoparticles self-assembled from trimethyl chitosan and fucoidan for enhanced oral delivery of insulin. Int J Biol Macromol. 2018;126:141–150. https://doi.org/10.1016/j.ijbiomac.2018.12.182.

التصنيع الاخضر وتوصيف الجسيمات النانوية من يوديد النحاس (CuI) المحضرة باستخدام مستخلص الملفوف الأحمر.

اماني سمير عبد السادة[1]، زينب جاسم شنان[1]، عقيل مشحوت جعفر[2]

[1] قسم الفيزياء، كلية العلوم للبنات، جامعة بغداد ، العراق.
[2] دائرة الطاقات المتجددة، مركز الطاقة الشمسية، وزارة التعليم العالي والبحث العلمي/ العلوم والتكنولوجيا، بغداد ، العراق.

الخلاصة

تعد جسيمات يوديد النحاس النانوية (CuI NPs) واحدة من المواد الواعدة للاستخدام في العديد من التطبيقات الإلكترونية. في هذا العمل، تم تحضير جسيمات نانوية شفافة من CuI بواسطة التصنيع بالطريقة الخضراء، والذي تم بواسطة مستخلص الملفوف الأحمر المستخدم ليس فقط كعامل مختزل ولكن أيضًا كعامل حجب لتقليل السمية في تحضير الهياكل النانوية CuI. تم دراسة الخواص التركيبية باستخدام تقنية تحليل حيود الأشعة السينية (XRD). أظهر تحليل الأشعة السينية أن الهيكل ذو طبيعة متعددة البلورات مع طور مكعب ويظهر اتجاه المستوى البلوري على طول المستوى (111). تم استخدام مجهر القوة الذرية (AFM) لفحص معلمات السطح المجهري للغشاء الرقيق CuI لفحص وقياس التشكل ومتوسط القطر والخشونة. تم تأكيد القياسات البصرية بواسطة UV-Visible، والتي أظهرت أن الجسيمات النانوية CuI لديها فجوة طاقة بانتقال الكتروني مسموح وبشكل مباشر وتغير في الامتصاص إلى طول موجة أقصر (إلى منطقة تحول الطول الموجي للأشعة فوق البنفسجية). تم التحقق من التحليل الطيفي للأشعة تحت الحمراء لتحويل فورييه (FT-IR) من وجود روابط C=O وNO-O وCH، وتؤكد هذه الدراسة القدرة العالية على الاختزال وحجب الجزيئات النانوية لـ CuI NPs عبر الجزيئات الحيوية الموجودة في المستخلص النباتي. أظهر تحليل المجهر الإلكتروني لمسح الانبعاث الالكتروني (FE-SEM) شكل الـ CuI NPs، وأظهرت النتائج أن صور جسيمات يوديد النحاس النانوية المنتجة تبدو وكأنها صفائح من رقائق مثلثة. تمت دراسة نمط توزيع حجم جسيمات CuI NPs واستقرارها باستخدام محلل زيتا. كشف تحليل جهد زيتا عن احتمالية تبلغ -5.08 مللي فولت مما يدل على ضعف الاستقرار بسبب تراكم المادة.

الكلمات المفتاحية: يوديد النحاس، التصنيع الأخضر، مستخلص الملفوف الأحمر, الخصائص التركيبية، الخصائص البصرية.